Tyrosine Replacing Tryptophan as an Anchor in GWALP Peptides

ARTICLE *in* BIOCHEMISTRY · MARCH 2012

Impact Factor: 3.02 · DOI: 10.1021/bi201732e · Source: PubMed

Published in final edited form as:
Biochemistry. 2012 March 13; 51(10): 2044–2053. doi:10.1021/bi201732e.

Tyrosine Replacing Tryptophan as an Anchor in GWALP Peptides†

Nicholas J. Gleason[1], **Vitaly V. Vostrikov**[1], **Denise V. Greathouse**[1], **Christopher V. Grant**[2], **Stanley J. Opella**[2], and **Roger E. Koeppe II**[1,*]

[1]Department of Chemistry and Biochemistry, University of Arkansas, Fayetteville, AR 72701

[2]Department of Chemistry and Biochemistry, University of California, San Diego; La Jolla, CA 92093

Abstract

Synthetic model peptides have proven useful for examining fundamental peptide-lipid interactions. A frequently employed peptide design consists of a hydrophobic core of Leu-Ala residues with polar or aromatic amino acids flanking each side at the interfacial positions, which serve to "anchor" a specific transmembrane orientation. For example, WALP family peptides (acetyl-GWW$(LA)_n$LWWA-[ethanol]amide), anchored by four Trp residues, have received particular attention in both experimental and theoretical studies. A recent modification proved successful in reducing the number of Trp anchors to only one near each end of the peptide. The resulting GWALP23 (acetyl-GGALW^5$(LA)_6$LW^{19}LAGA-[ethanol]amide) displays reduced dynamics and greater sensitivity to lipid-peptide hydrophobic mismatch than traditional WALP peptides. We have further modified GWALP23 to incorporate a single tyrosine, replacing W^5 with Y^5. The resulting peptide, Y^{5}GWALP23 (acetyl-GGALY^5$(LA)_6$LW^{19}LAGA-amide) has a single Trp residue that is sensitive to fluorescence experiments. By incorporating specific ^{2}H and ^{15}N labels in the core sequence of Y^{5}GWALP23, we were able to use solid-state NMR spectroscopy to examine the peptide orientation in hydrated lipid bilayer membranes. The peptide orients well in membranes, and gives well defined ^{2}H quadrupolar splittings and ^{15}N/^{1}H dipolar couplings throughout the core helical sequence between the aromatic residues. The substitution of Y^5 for W^5 has remarkably little influence on the tilt or dynamics of GWALP23 in bilayer membranes of the phospholipids DOPC, DMPC or DLPC. A second analogue of the peptide with one Trp and two Tyr anchors, Y^{4,5}GWALP23, is generally less responsive to the bilayer thickness and exhibits lower apparent tilt angles with evidence of more extensive dynamics. In general, the peptide behavior with multiple Tyr anchors appears to be quite similar to the situation when multiple Trp anchors are present, as in the original WALP series of model peptides.

Keywords

deuterium and ^{15}N solid-state NMR; lipid bilayer; GALA analysis; PISEMA

†This work was supported in part by NSF grant MCB 0841227 and by the Arkansas Biosciences Institute. The peptide facility is supported by NIH grants RR31154 and RR16460. The NMR facilities are supported by NIH grant RR31154 and the Biotechnology Research Center for NMR Molecular Imaging of Proteins at the University of California, San Diego, which is supported by NIH grant P41EB003031.

Address correspondence to: Roger E. Koeppe II, Tel. (479) 575-4976; Fax. (479) 575-4049; rk2@uark.edu.

Supporting Information Available. Chromatogram, mass spectra, and additional NMR and fluorescence spectra for characterization of peptides and lipids. This material is available free of charge via the Internet at http://pubs.acs.org.

Because characterizing the structures and functional properties of membrane proteins is generally a more complicated task than for aqueous soluble proteins, synthetic model membrane peptides have proven to be valuable for discerning fundamental principles that govern protein-lipid interactions. These chemically well-defined peptide systems offer opportunities for examining direct lipid interactions by placing limits upon external factors such as multiple transmembrane helices, large steric effects or interactions in oligomers. One of the first such peptide sequences was acetyl-KK$(L)_{24}$KK-amide (1, 2). This sequence was chosen because it consists of a hydrophobic poly-leucine α-helix that was expected to associate with the acyl chains in a lipid bilayer membrane flanked on the ends by two hydrophilic, charged lysine residues that are expected to be soluble in the aqueous environment adjacent to the membrane. In this and other model membrane-spanning peptides, the N- and C- termini generally are capped to render them uncharged. Later peptide models incorporated an interior helical $(Leu\text{-}Ala)_n$ core sequence, which resulted in a lower overall hydrophobicity and an increased sensitivity to the identities of the lipids that compose the bilayer (3).

A survey of type I single-span membrane proteins revealed a non-random distribution of the aromatic Trp, Tyr and Phe residues (4). These aromatic residues are typically located near the aqueous-lipid interface where they are believed to act as anchors to help position the transmembrane helix within the bilayer (5). Other experiments with gramicidin A revealed that the Trp preference for the membrane interfacial region promotes lipid H_{II} phase formation (6), as well as assembly of dimeric gramicidin channels in lipid bilayer membranes (7). WALP peptides (acetyl-GWWA$(LA)_n$LWWA-[ethanol]amide) incorporating multiple Trp anchors and the helical, hydrophobic repeating Leu-Ala core sequence induced lipid phase changes, similar to gramicidin A, as a function of lipid-peptide hydrophobic mismatch (8). Later the four Trp anchor residues were mutated to various other aromatic or charged residues (Tyr, Phe, Lys, Arg, or His) to monitor the importance of the anchor's chemical and physical properties (9, 10). These model peptides helped to describe the properties, such as peptide-dependent lipid phase behavior and lipid ordering, caused by the hydrophobic mismatch. In 2002, it was reported that WALP peptides have a characteristic non-zero tilt with respect to a lipid bilayer normal (11); on theoretical grounds the fundamental tilt subsequently was attributed to the entropy of precession about the bilayer normal (12). The ability to decrease the number of anchor residues has been demonstrated with (acetyl-GGALW$(LA)_6$LWLAGA-[ethanol]amide), which possesses only one Trp anchor near each of the termini (13). The tryptophans in GWALP23 flank a hydrophobic Leu-Ala core of the same length as that of WALP19 (8, 11). With fewer anchor residues, it becomes easier to assess the roles of each of them. For example, the measured ^2H quadrupolar splittings and apparent tilt angle of GWALP23 in lipid bilayers are much more responsive than those of WALP19 or WALP23 to the lipid hydrophobic thickness (14). Furthermore, the average tilt direction of GWALP23 remains essentially constant in lipid bilayers of different thickness (14). These results suggest that the four Trp anchors in the original WALP series of peptides are so dominating that they induce significant peptide dynamics, and variations in the tilt direction (14), while resisting significant changes to the magnitude of the apparent average tilt angle, even in cases where the bilayer thickness changes.

A further step beyond GWALP23 would be to replace one of the two remaining tryptophans with another chemically different anchoring residue. An advantage of such an approach would be to open a window for fluorescence experiments involving the single remaining Trp residue. To this end, we have investigated the influence of a single Trp to Tyr replacement upon GWALP23. The choice of tyrosine is based upon our preference to retain an aromatic residue and an uncharged "host" peptide (in preparation for future experiments that could investigate the introduction of a variety of "guest" charged residues within a parent peptide).

We have synthesized a new peptide Y^5GW^{19}ALP23 (acetyl-GGALY$(LA)_6$LWLAGA-amide) and have incorporated deuterated alanine residues and ^{15}N-labeled residues in selected sequence positions for analysis by solid-state NMR. Using circular dichroism spectroscopy, solid-state ^{2}H NMR spectroscopy with "Geometric Analysis of Labeled Alanines" (GALA) (11), and solid-state ^{15}N/^{1}H high resolution separate local field NMR spectroscopy (15, 16), we have characterized the properties of Y^5GW^{19}ALP23 in lipid bilayer membranes of DOPC, DMPC and DLPC. Additionally, we incorporated a second tyrosine to form $Y^{4,5}GW^{19}$ALP23 and compared the orientation and dynamics of the "double-tyrosine" anchored peptide with those of Y^5GW^{19}ALP23 in the three different lipid bilayer membranes.

Knowledge of the orientations and dynamics of model transmembrane helices is significant for understanding principles that undergird not only the structure and function of membrane proteins in general but also the mechanisms of signaling (17, 18). To this end, it is important to have robust model systems that will establish a vigorous framework for such understanding.

Materials and Methods

Solid Phase Synthesis of ^{2}H-Labeled Peptides

Commercial L-alanine-d_4 from Cambridge Isotope Laboratories (Andover, MA) was modified with an Fmoc group, as described previously (19), and recrystallized from ethyl acetate:hexane, 80:20. NMR spectra (^{1}H) were used to confirm successful Fmoc-Ala-d_4 synthesis. Fmoc-L-Ala-^{15}N and Fmoc-L-Leu-^{15}N were purchased from Cambridge. Other protected amino acids and acid-labile "Rink" amide resin were purchased from NovaBiochem (San Diego, CA). All peptides were synthesized on a 0.1 mmol scale using "FastMoc™" methods and a model 433A synthesizer from Applied Biosystems by Life Technologies (Foster City, CA). Typically, two deuterated alanines of differing isotope abundances were incorporated into each synthesized peptide. Selected precursors for deuterated residues therefore contained either 100% Fmoc-L-Ala-d_4 or 60% Fmoc-L-Ala-d_4 with 40% non-deuterated Fmoc-L-Ala. Some peptides were synthesized without deuterium, but with 100% abundance of ^{15}N in selected residues. The final residue on each peptide was acetyl-Gly to yield a blocked, neutral N-terminal.

A peptide cleavage solution was prepared containing 85% trifluoroacetic acid (TFA) and 5% each (v/v or w/v) of triisopropylsilane, water, and phenol. TFA cleavage from "Rink" resin in 2 mL volume (2–3 h at 22 °C) leads to a neutral, amidated C-terminal. Peptides were precipitated by adding the TFA solution to 25 volumes of cold 50/50 MtBE/hexane. Peptides were collected by centrifugation, washed multiple times with MtBE/hexane, and lyophilized multiple times from (1:1) acetonitrile/water to remove residual TFA. MALDI-TOF mass spectrometry was used to confirm peptide molecular mass (Figure S1 in Supplementary Material). Peptide purity was examined by reversed-phase HPLC with 280 nm detection, using a 4.6 × 50 mm Zorbax SB-C8 column packed with 3.5 μm octyl-silica (Agilent Technologies, Santa Clara, CA), operated at 1 mL/min using a methanol/water gradient from 85% to 99% methanol (with 0.1% TFA) over five min (Figure S2 in Supplementary Material). Peptide amounts were measured by means of UV absorbance at 280 nm, using molar extinction coefficients of 5,600 M^{-1} cm^{-1} for each Trp and 1,490 M^{-1} cm^{-1} for each Tyr residue in the peptide (20). Solvents were of the highest available purity. Water was doubly deionized Milli-Q™ water.

^{2}H NMR Spectroscopy using Oriented Bilayer samples

Mechanically aligned samples for solid-state NMR spectroscopy (1/60, peptide/lipid) were prepared using DOPC, DMPC or DLPC lipids from Avanti Polar Lipids (Alabaster, AL), and deuterium-depleted water (Cambridge; 45% w/w hydration), as described previously (11). Bilayer alignment within each sample was confirmed using ^{31}P NMR at 50 °C on a Bruker Avance 300 spectrometer (Billerica, MA) at both $\beta = 0°$ (bilayer normal parallel to magnetic field) and $\beta = 90°$ macroscopic sample orientations (Figure S3 in Supplementary Material). Deuterium NMR spectra were recorded at 50 °C using both sample orientations on a Bruker Avance 300 spectrometer, utilizing a quadrupolar echo pulse sequence (21) with 90 ms recycle delay, 3.2 μs pulse length and 115 μs echo delay. Between 0.6 and 1.5 million scans were accumulated during each ^{2}H NMR experiment. An exponential weighting function with 100 Hz line broadening was applied prior to Fourier transformation.

^{15}N NMR Spectroscopy using Magnetically Oriented Bicelles

Magnetically oriented bicelles for solid-state ^{15}N NMR spectroscopy (1/80, peptide/total lipid) were prepared using DMPC-ether and DHPC-ether lipids (3.2/1.0, mol/mol; “q” value) from Avanti Polar Lipids (Alabaster, AL), in a total volume of 175 μL deuterium-depleted water (Cambridge). Peptide and DHPC-ether were mixed and then dried under nitrogen flow and vacuum to remove organic solvent. Separate samples of the separate DMPC-ether lipid also were prepared in aliquots and dried. Peptide/DHPC-ether films were hydrated using 100 μL water, and DMPC-ether with 75 μL water. After the contents of two separate vials were soluble, the peptide/DHPC-ether solution was transferred to the DMPC-ether solution. Contents were cycled between 0 °C and 45 °C several times, with intermittent vortexing, until the solution remained clear when cold. While still cold, the bicelle sample solution was transferred to a 5 mm NMR tube and sealed.

For ^{15}N-based SAMPI4 experiments (in the same family of pulse sequences as PISEMA), GWALP23 and Y^{5}GWALP23 enriched in ^{15}N leucine and alanine were synthesized (five labels, residues 13–17). ^{15}N chemical shifts and ^{15}N-^{1}H dipolar coupling values were recorded using 500 MHz Bruker Avance and Varian Inova spectrometers and established pulse sequences (15),(22, 23) (24). Solid-state NMR high resolution separated local field SAMPI4 experiments (25) were performed using a 1 ms CP contact time, RF field strengths of approximately 50 kHz; 54 t1 points were acquired using 8.0 ms of acquisition time in the direct (t2) dimension and a 7.5 s recycle delay. The sample temperature was maintained at 42 °C, just below a critical temperature for structural transformation of DMPC/DHPC bicelle samples (26). We have found that the peptide order parameter is essentially unchanged between DMPC/DHPC bicelles at 42 °C and bilayer plate samples at 50 °C (27), where the spectral quality often improves for the plate samples (28). Attempts were made also to construct DLPC-based “bicelles” using DLPC-ether, DHPC-ether, and dipentanoyl-PC (13.3/3/1) with peptide incorporated at 1/80 (peptide/DLPC; mol/mol) (29). Unfortunately, initial efforts did not yield well oriented bicelles; thus we were unable to resolve the ^{15}N/^{1}H dipolar couplings or assign the ^{15}N chemical shift frequencies for such samples using the ^{15}N-based SAMPI4 experiments.

Data Analysis

Combinations of ^{2}H quadrupolar splittings and ^{15}N/^{1}H dipolar coupling frequencies, individually or together, and in some cases along with ^{15}N chemical shift values, were used to calculate the orientations of the peptide helix in the bilayers. Data uncertainty was estimated to be within ±0.5 kHz based on duplicate samples and measurements using different orientations of glass slide samples (27). We performed calculations both with a semi-static (variable S_{zz}) model (30) and with a more dynamic model that incorporates

Gaussian distributions for the tilt and direction of tilt (30). The detailed strategy for combined ^{2}H and $^{15}N/^{1}H$ analysis has been described (27).

The analysis using semi-static peptide dynamics involves a principal order parameter S_{zz} to estimate overall peptide motion with respect to an apparent average peptide orientation. These calculations are based on the GALA analysis, as previously described (11, 30, 31). For samples in DMPC, we incorporate also $^{15}N/^{1}H$ dipolar coupling and ^{15}N chemical shift values obtained from SAMPI4 spectra, to determine a best fit to the experimental data (32). These calculations are performed using helix tilt τ, rotation ρ about the helix axis and a principal order parameter S_{zz} as variable parameters. The analysis takes into account the ^{2}H quadrupolar splittings and/or $^{15}N/^{1}H$ dipolar coupling frequencies and ^{15}N chemical shifts for the isotope-labeled residues based on ideal α-helix geometry.

To proceed beyond a semi-static model, we performed calculations that take into account more complex peptide dynamics, in which σ_τ and σ_ρ relate to the widths of Gaussian distributions for the peptide tilt and rotation (30). In this analysis, a principal order parameter S_{zz} is fixed at 0.88 to reflect isotropic fluctuations; and further anisotropic variations in τ and ρ are permitted. A best-fit RMSD to observed dipolar and quadrupolar couplings, and ^{15}N chemical shift values, is based upon the parameters τ_o, ρ_o, σ_τ and σ_ρ., following (30). Fixed parameters in the analysis included chemical shift tensor components (σ_{11}, σ_{22}, σ_{33}) of (64, 77, 224) ppm, as reported for model dipeptides (33) and small proteins (34); a coupling constant of 10.22 kHz (based on an NH bond length of 1.06 Å) (35, 36); and the angle $\varepsilon_{//}(14°)$ between the peptide helix axis and the N-H bond. In the combined analysis, equal weights were assigned to the ^{2}H methyl quadrupolar couplings, $^{15}N/^{1}H$ dipolar coupling frequencies, and the ^{15}N chemical shift frequencies. Further details are described in (27) and (37).

CD Spectroscopy

Small lipid vesicles incorporating 125 nM peptide and 7.5 μM lipid (1/60) were prepared by sonication in unbuffered water. An average of ten scans was recorded on a Jasco (Easton, MD) J710 CD spectropolarimeter, using a 1 mm cell path length, 1.0 nm bandwidth, 0.1 nm slit and a scan speed of 20 nm/min.

Steady-state Fluorescence Spectroscopy

Vesicle solutions with 1/60 peptide/lipid for fluorescence experiments were prepared by dilution, 1/20 with water, of the samples prepared previously for CD spectroscopy (above). Samples were excited at 280 nm or 295 nm with a 5 nm excitation slit, and emission spectra were recorded between 300 and 420 nm with a 5 nm emission slit using a Hitachi F-2500 fluorescence spectrophotometer. The spectra from five scans were averaged.

Results

Synthetic WALP peptides as well as analogues such as GWALP23 possess primarily α-helical character that is typical of transmembrane segments, and is expected from the repeating Leu-Ala core residues, which possess a propensity for forming helices. When the $L^{4}W^{5}$ sequence of GWALP23 is replaced with $L^{4}Y^{5}$ or $Y^{4}Y^{5}$, the resulting peptides have “single” or “double” Tyr anchors N-terminal to the core $(Leu\text{-}Ala)_n$ sequence. Circular dichroism spectra for such peptides in lipid bilayer membranes demonstrate equal or slightly reduced α-helical character when the Tyr anchor(s) are present, compared to GWALP23 (Figure 2). In particular, the presence of Y^{4} as a second “anchor” residue seems to have little influence on the CD spectrum or the magnitudes of the peaks that characterize α-helices. Importantly, both the Y^{5} and $Y^{4,5}$ derivatives maintain primarily an α-helical backbone

structure. With sample formulation being vesicles for the CD spectra, stacked bilayers for the ^{2}H NMR spectra and bicelles for the ^{15}N/^{1}H NMR spectra, we believe that the core domains of the peptides are helical in all of the lipid membrane environments. Indeed, the ^{2}H resonances show agreement between bicelles and bilayers (27), and follow a helical pattern for the core alanines, while also illustrating helix unwinding in the vicinity of A^{3} and A^{21}, outside of the central core sequence (14).

Further information was obtained from oriented lipid bilayer samples that included the ^{2}H-labeled Tyr-containing peptides at a peptide:lipid molar ratio of 1:60. For such samples, ^{31}P NMR spectra confirmed that the bilayers were well aligned with respect to the magnetic field (Supporting Information, Figure S3). For the $\beta = 90°$ sample orientation, a strong single ^{31}P resonance was observed at ~ −24 ppm (with the precise chemical shift frequency varying from −22.4 ppm to −26.3 ppm in the DLPC, DMPC and DOPC lipid bilayer membranes). When samples were oriented at $\beta = 0°$, a strong peak at ~ +18 ppm was observed as well as small amounts of unoriented lipids that comprised a minor peak around −24 ppm.

The ^{2}H NMR spectra display the two expected pairs of resonances corresponding to the quadrupolar splittings from the two labeled Ala methyl side chains in each peptide. Figure 3 includes the spectra for alanines 7 and 17 in GWALP23, Y^{5}GWALP23, and $Y^{4,5}$GWALP23, each incorporated in DLPC, DMPC and DOPC bilayer membranes. The spectra for the other labeled alanines are included as supplemental material (Figures S4–S5). In rare cases, single sets of broad peaks were observed due to spectral overlap arising from similar ^{2}H quadrupolar splittings from the two alanines. When the plate samples are turned from the $\beta = 0°$ orientation to $\beta = 90°$, the quadrupolar splittings are found to be reduced by a factor of two. The appearance of sharp resonances with half-magnitude quadrupolar splittings at $\beta = 90°$ illustrates that the peptides undergo fast axial rotational diffusion about the bilayer normal on the NMR timescale (38). It should be noted that the fast rotational averaging about the precession axis (bilayer normal) is distinct from averaging about the helix axis which, if complete, could average all of the ^{2}H Ala signals to a common value (11), contrary to what is observed.

Y^{5}GWALP23 produced a relatively large range of ^{2}H quadrupolar splitting magnitudes, from 8 kHz up to 30 kHz in DLPC (Table 2), suggesting a significant tilt of the peptide helix with respect to the bilayer normal. Somewhat smaller ranges of 4–23 kHz and 1–17 kHz were observed for Y^{5}GWALP23 in DMPC and DOPC, respectively. It is also noteworthy that the quadrupolar splittings for Y^{5}GWALP23 are in each case within 0.1 to 4 kHz of the corresponding Ala CD_3 signals in GWALP23 (14), suggesting that the Y^{5} and W^{5} peptides may adopt similar membrane orientations.

In contrast, the double-anchored $Y^{4,5}$GWALP23 exhibits a much smaller range of quadrupolar splittings, varying only between 1 kHz and 12 kHz in all three lipid bilayers (Table 2). The signals from $Y^{4,5}$GWALP23 do not appear to be similar to those from GWALP23 or Y^{5}GWALP23 in any of the lipid systems. Additionally, the range of quadrupolar splitting frequencies for $Y^{4,5}$GWALP23 remains approximately the same in each type of lipid bilayer membrane, regardless of the bilayer thickness. The quadrupolar splitting magnitudes for each of the six core alanine methyl side chains in Y^{5}GWALP23 and $Y^{4,5}$GWALP23 are listed in Table 2 for each of the DLPC, DMPC and DOPC bilayer membrane environments.

Additional orientation information was derived from ^{15}N-based SAMPI4 experiments that utilized magnetically aligned peptide-containing bicelles composed of the ether analogues of DMPC and DHPC (q=3.2:1, mol:mol). In these experiments, similar ranges are observed for

the ^{15}N chemical shift frequencies of residues 13–17 in GWALP23 (85 ppm to 100.7 ppm) and Y^{5}GWALP23 (84 ppm to 101 ppm; see Table 3). While the corresponding ^{15}N/^{1}H dipolar coupling frequencies also are very similar, the ones for Y^{5}GWALP23 are slightly yet systematically smaller in magnitude (0.2 kHz to 0.5 kHz) than those for GWALP23, resulting in a SAMPI4 spectrum that appears to be somewhat below that of GWALP23 (Figure 4).

Tilt magnitude, direction and dynamics of Y^{5}GWALP23

For Y^{5}GWALP23 in DMPC, we utilized a combined analysis of available data from ^{2}H and ^{15}N solid-state NMR experiments (27, 37), using Gaussian as well as semi-static treatments of the dynamics. For the DMPC environment, we have a large collection of six ^{2}H-Ala methyl quadrupolar splitting magnitudes, together with the ^{15}N chemical shift frequencies and ^{15}N/^{1}H dipolar coupling frequencies from residues 13–17 (Fig 3–4; Tables 2–3), giving a total of 16 restraints. For the DLPC environment, we calculated Gaussian and semi-static fits to the dynamics using the six ^{2}H-Ala methyl quadrupolar splittings from macroscopically oriented DLPC bilayers (Table 2; Fig 3).

The fits from the combined analysis of the ^{2}H and ^{15}N/^{1}H NMR data are quite good, with only minor discrepancies between the independent data sets (Figure 5; see Discussion). Importantly, the overall RMSD values of about 1.2 kHz (Table 4) from the combined fits are consistent with the uncertainty of the experimental measurements and suggest no over-fitting of the data. The quadrupolar and dipolar wave plots (Figure 5A, B) appear similar for the Gaussian and semi-static analysis methods, with data points close to the analytical curves that result from the combined analysis. Taken together, the independent measurements and the overall agreement lend confidence to the deduced molecular orientations and dynamics for the transmembrane peptides. The influence of the dynamics is evident from the ~10° smaller best-fit τ_o for the semi-static as opposed to the Gaussian analysis (Figure 5C). As has been characterized for other derivatives of GWALP23 (27), four closely spaced minima are observed for the best-fit values of (σ_τ,σ_ρ) (Figure 5D), with each minimum giving similar estimates for τ_o and ρ_o.

The dynamics as well as the average orientation of Y^{5}GWALP23 and GWALP23 are very similar in DMPC bilayers, regardless of whether Gaussian or semi-static approximations are employed to represent the peptide dynamics (Table 4). In DMPC, the Y5 and W5 peptides show similar small σ_τ values (5°–10°) and similar moderate to large σ_ρ values (65°–70°). The apparent tilt angles for the two peptides in DMPC also are nearly identical; namely τ_o for both the Y5 and W5 peptides is about 21° based on the Gaussian analysis, or about 10° smaller ("apparent" tilt magnitude) when using the semi-static analysis (which ignores σ_ρ; Table 4). Again comparing anchor residue Y5 to W5, the direction of peptide tilt ρ_o differs consistently by about 10° (Table 4), regardless of the method of analysis, or whether the host lipid bilayer is DMPC or DLPC.

In DLPC, the dynamics and average orientation of Y^{5}GWALP23 and GWALP23 are also very similar (Table 4). In these cases the Gaussian and semi-static fits to the dynamics, based on six ^{2}H quadrupolar splittings for each, yield similar τ_o values (about 21°). The Gaussian parameters in DLPC are modest, about 15° for σ_τ and about 30 for σ_ρ. Notably the helix properties do not vary when W5 is changed to Y5 in the GWALP23 framework in DLPC.

In DOPC bilayers, semi-static calculations performed using six ^{2}H quadrupolar splittings yield apparent tilt angles of about 6° for both Y^{5}GWALP23 and GWALP23 (Table 5). The overall trends are similar for both peptides, with the apparent tilt angles being smaller in DOPC than in DMPC. The direction of tilt ρ_o increases marginally and in parallel by about

5° from DLPC to DMPC, and by about 10° from DMPC to DOPC (Table 5), for both GWALP23 and Y^5GWALP23. Notably, therefore, the rotation of Y^5GWALP23 about its helix axis, ranging from about 295° in DLPC to 311° in DOPC, relative to the reference Cα of G^1 (11), is approximately a constant 10° less than that of GWALP23 in each lipid. The Tyr- and Trp-anchored peptide Y^5GWALP23, indeed, is found to behave very similarly to the original GWALP23 in possessing an adjustable tilt that is sensitive to the lipid membrane thickness. Figures 6A and 7A illustrate the rather similar ρ_o values for Y^5GWALP23 in bilayers of different thickness, along with the τ_o values that increase as the bilayer becomes thinner.

Increased dynamics for $Y^{4,5}$GWALP23

When a second tyrosine residue is introduced, in addition to the single Trp near the C-terminus, $Y^{4,5}$GWALP23 is found to behave quite differently from GWALP23 and Y^5GWALP23, as indicated first of all by the smaller range of observed ^{2}H quadrupolar splittings (Figure 2). Based on precedents with WALP23, and with the related peptide acetyl-GWALW$(LA)_6$LWLAWA-[ethanol]amide (WWALP23), the rather narrow range of ^{2}H quadrupolar splittings strongly suggests increased motional averaging of the ^{2}H signals (14, 27, 39, 40). Both the semi-static fit (with S_{zz} of 0.66) and the Gaussian fit (with σ_τ of 27°) indicate a regime of high dynamics for $Y^{4,5}$GWALP23 in DLPC (Table 4). In the other lipids, consistently low apparent τ_o values, together with apparent ρ_o values that diverge from bilayer to bilayer (Figures 6B, 7B; Table 5), again suggest highly dynamic behavior. Indeed the trends for $Y^{4,5}$GWALP23 mirror those that have been observed previously for WALP23 (31) and WWALP23 (14). Also WALP19 is seen to be highly dynamic (large σ_ρ value) in DLPC (41), although a model-dependent analysis (in which σ_τ is set to zero) suggests that low values of σ_ρ may be allowed under conditions of negative mismatch (41).

Opening the fluorescence window

An added advantage of Y^5GWALP23 is the presence of only a single Trp residue, whose emission λ_{max} should be unambiguously sensitive to the polarity of the environment of the single indole ring (42). It is within this context important to confirm that the fluorescence emission from Y^5GWALP23 is characteristic of interfacial tryptophan. Indeed, when Y^5GWALP23 and $Y^{4,5}$GWALP23 are excited at 295 nm, so as to minimize the contributions from the tyrosines, their emission spectra closely overlap that of GWALP23 (Figure 8), with λ_{max} being about 335 nm for each peptide. The results suggest similar interfacial locations for the Trp residue(s) in all three peptides. When the excitation wavelength is 280 nm, contributions from the Tyr residue(s) are evident (Figure S6 of the Supporting Information). (The Tyr fluorescence emission [at 306 nm], unlike the case of Trp, is not dependent on environment polarity.) The spectra in Figure 8 moreover suggest that fluorescence from Y^5GWALP23, excited at 295 nm, can serve as an effective probe for potential helix (center-of-mass) translation with respect to the bilayer midplane under the influence of guest residues. For example, when a guest arginine is introduced at position 14 in GWALP23, such helix translation by about 3 Å has been predicted by coarse-grained molecular dynamics simulations (43), but has not yet been observed experimentally.

Discussion

How many Trp residues are needed to maintain a defined orientation, with moderate to low dynamics, and minimal aggregation, for a transmembrane helical domain relative to an interface between water and the interior of a lipid bilayer membrane? Gramicidin channels have eight tryptophans (7), while the original WALP peptides employ only four tryptophans (8). With the introduction of GWALP23 (13), we found that as few as two Trp residues can

define a preferred orientation for a transmembrane α-helix (14). Now with the replacement of W5 by Y5, we learn that one interfacial Trp and one interfacial Tyr can confer a stable transmembrane orientation for Y^5GWALP23. Remarkably, the extent of dynamic averaging of the NMR resonances is *less* when only two Trps—or one Trp and one Tyr—are present than when more than two interfacial aromatic residues are present. In particular, the dynamic averaging is very extensive, and involves especially large values of σ_ρ, when four Trps (WALP23 and WWALP23; (14)) or one Trp with two Tyr ($Y^{4,5}$GWALP23; this work) provide the interfacial anchoring. Aspects of the data analysis and of the consequences of tyrosine substitutions for the orientation and dynamics of GWALP23 will be discussed in turn.

Agreement of independent solid-state NMR methods

We took advantage of the combined and simultaneous analysis of ^{2}H quadrupolar splittings, ^{15}N chemical shifts and ^{15}N/^{1}H dipolar couplings for Y^5GWALP23 in DMPC. The combined goodness-of-fit is essentially the same for GWALP23 and Y^5GWALP23, giving RMSD values of about 1.2 kHz when 16 parameters are analyzed for either of the peptides in DMPC (Table 4). With smaller data sets involving only a single type of parameter, the apparent RMSD values are somewhat lower, typically near 0.6 kHz; yet the deduced values of τ_o and ρ_o are essentially the same. For example, semi-static analysis gives a (τ_o, ρ_o) estimate of (10°, 300°) when the six ^{2}H $\Delta\nu_q$ values are analyzed alone (Table 5), compared to (16°, 306°) for the set of five ^{15}N chemical shifts and five ^{15}N/^{1}H dipolar couplings, or (12°, 298°) when all sixteen data points are employed (Table 4). As noted previously (13), the independent solid-state NMR methods agree rather well.

Similar behavior is observed for GWALP23 and its W5 → Y5 analogue

GWALP23 and Y^5GWALP23 show similar orientations and dynamics in DLPC, DMPC and DOPC bilayer membranes (Tables 4–5). Remarkably, either a single tyrosine or a single tryptophan at position 5 is sufficient to define the orientation of the N-terminal of the transmembrane peptide with respect to W19 as the sole anchor for the C-terminus. For both peptides in DMPC, the Gaussian dynamic fits show small values of σ_τ (5°–10°) and moderate values of σ_ρ (65°–70°) (Table 4). Indeed, if one compares in detail the fits to the Gaussian dynamics in DMPC (Figure 9), the similar narrow distributions of τ, and broad distributions of ρ, for the two peptides can be directly observed. Notably, the most probable τ_o is identical for the two peptides (Figure 9), while the width of the τ distribution increases marginally when Y5 is present, leading to the small increase in σ_τ from ~5° to ~10° for Y^5GWALP23 (Table 4). We performed Gaussian analysis also for the peptides in DLPC, using the ^{2}H NMR data (Table 4). Once again, the results for Y^5GWALP23 agree with those for GWALP23 itself. In DLPC, the Gaussian and semistatic analyses return nearly equivalent values of τ_o, in the range of 19°–23° for both peptides, and the ~10° offset in ρ_o is maintained between W5 and Y5. The Gaussian analyses indicate moderate values of about 30° for σ_ρ and about 15° for σ_τ for GWALP23 and Y^5GWALP23 in DLPC (Table 4). Importantly, apart from the 10° change in ρ_o, the Gaussian distributions remain essentially the same when the identity of residue five is modified from Trp to Tyr.

The semi-static fits to the ^{2}H NMR data reveal similar apparent tilt angles for the W5 and Y5 peptides in DOPC, as well as in DMPC and DLPC (Table 5). In all three lipids, the main effect of Y5 is to alter the most probable direction of the peptide tilt ρ_o by about 10° (Tables 4–5), a result which is independent of whether a semi-static or Gaussian analysis is used to estimate the dynamics. GWALP23 and Y^5GWALP23 exhibit, furthermore, less extensive motional averaging of their ^{2}H and ^{15}N resonances than WALP23 (30) or WWALP23 (14) in each of the lipid membranes. With this direct comparison of residues W5 and Y5 in

GWALP23 now available, it would be of future interest to compare also the substitution of W19 with Y19.

Enhanced dynamics when Y4 is introduced into Y^5GWALP23

To address the question of whether one or two Tyr residues would be preferable for defining a transmembrane helix orientation, we compared the properties of the Y5 and Y4,5 peptides. The comparison (Figures 6–7) indicates a loss of systematic behavior when Y4 is introduced alongside Y5. With Y4 present, the observed ^{2}H $\Delta\nu_q$ magnitudes span only a small range in each lipid, ρ_o becomes unpredictable in membranes of different thickness, and τ_o no longer scales with the bilayer thickness. Indeed, the dynamic properties of $Y^{4,5}$GWALP23, as revealed by ^{2}H NMR, resemble those of WALP19 (11, 12), $W^{(2,3,21,22)}$ALP23 (30, 31, 39, 40, 44, 45), and $W^{2,22}W^{5,19}$ALP23 (14), all of which possess 4 Trp residues. It is nevertheless conceivable that also the loss of the hydrophobic L4 residue itself could contribute to the apparent changes in the peptide dynamics, a situation which could be checked by investigating the properties of the single-tyrosine mutant Y^4GWALP23 peptide. Regardless of such a possibility, the present results suggest that “extra” aromatic residues may compete with each other at the membrane interface.

Summarizing perspective: implications for the number of interfacial aromatic residues

The accumulated results to date indicate, concerning the preferred number of aromatic Trp or Tyr residues to anchor each end of a transmembrane helix, that “one is enough,” and “two are too many.” When (W^5)GWALP23 and Y^5GWALP23 are compared, the orientations and dynamic properties are found to be remarkably similar in three different lipid bilayer membranes; namely Tyr is found to define a preferred peptide orientation as effectively as Trp (at the N-terminal). (The relative anchoring potential of Tyr versus Trp has yet to be established at the C-terminal.) Importantly, including additional aromatic residues—whether one more tyrosine in $Y^{4,5}$GWALP23, or two more tryptophans (for example, in WALP23 or WWALP23)—markedly increases the extent of the peptide dynamics. It is plausible that the increased dynamic behavior may be due to competition among different aromatic residues for preferred positions with respect to the head groups of the lipid bilayer.

Supplementary Material

Refer to Web version on PubMed Central for supplementary material.

Acknowledgments

We thank Marvin Leister for extensive help with the deuterium NMR experiments.

ABBREVIATIONS and FOOTNOTES

CD	circular dichroism
DLPC	1,2-dilauroylphosphatidylcholine
DMPC	1,2-dimyristoylphosphatidylcholine
DOPC	1,2-dioleoylphosphatidylcholine
DMPC-ether	1,2-di-O-myristoylphosphatidylcholine
DHPC-ether	1,2-di-O-hexylphosphatidylcholine
Fmoc	Fluorenylmethoxycarbonyl
GALA	Geometric analysis of labeled alanines

GWALP23	acetyl-GGALW$(LA)_6$LWLAGA-[ethanol]amide
MtBE	methyl-*t*-butyl ether
PISEMA	Polarization inversion spin exchange at magic angle
RMSD	root mean squared deviation
TFA	trifluoroacetic acid
WWALP23	acetyl-GWALW$(LA)_6$LWLAWA-[ethanol]amide

References

1. Davis JH, Hodges RS, Bloom M. The Interaction between a Synthetic Amphiphilic Polypeptide and Lipids. Biophys J. 1982; 37:170–171. [PubMed: 19431462]
2. Davis JH, Clare MD, Hodges RS, Bloom M. The Interaction between a Synthetic Amphiphilic Polypeptide and Lipids in a Bilayer Structure. Biochemistry. 1983; 22:5298–5305.
3. Zhang YP, Lewis RN, Henry GD, Sykes BD, Hodges RS, McElhaney RN. Peptide models of helical hydrophobic transmembrane segments of membrane proteins. 1. Studies of the conformation, intrabilayer orientation, and amide hydrogen exchangeability of Ac-K_2-$(LA)_{12}$-K_2-amide. Biochemistry. 1995; 34:2348–2361. [PubMed: 7857945]
4. Landolt-Marticorena C, Williams KA, Deber CM, Reithmeier RA. Non-random distribution of amino acids in the transmembrane segments of human type I single span membrane proteins. J Mol Biol. 1993; 229:602–608. [PubMed: 8433362]
5. Schiffer M, Chang CH, Stevens FJ. The functions of tryptophan residues in membrane proteins. Protein Eng. 1992; 5:213–214. [PubMed: 1409540]
6. Killian JA, Prasad KU, Urry DW, de Kruijff B. A mismatch between the length of gramicidin and the lipid acyl chains is a prerequisite for H_{II} phase formation in phosphatidylcholine model membranes. Biochim Biophys Acta. 1989; 978:341–345. [PubMed: 2464375]
7. O'Connell AM, Koeppe RE 2nd, Andersen OS. Kinetics of gramicidin channel formation in lipid bilayers: transmembrane monomer association. Science. 1990; 250:1256–1259. [PubMed: 1700867]
8. Killian JA, Salemink I, de Planque MR, Lindblom G, Koeppe RE 2nd, Greathouse DV. Induction of nonbilayer structures in diacylphosphatidylcholine model membranes by transmembrane alpha-helical peptides: importance of hydrophobic mismatch and proposed role of tryptophans. Biochemistry. 1996; 35:1037–1045. [PubMed: 8547239]
9. de Planque MR, Kruijtzer JA, Liskamp RM, Marsh D, Greathouse DV, Koeppe RE 2nd, de Kruijff B, Killian JA. Different membrane anchoring positions of tryptophan and lysine in synthetic transmembrane alpha-helical peptides. J Biol Chem. 1999; 274:20839–20846. [PubMed: 10409625]
10. de Planque MR, Boots JW, Rijkers DT, Liskamp RM, Greathouse DV, Killian JA. The effects of hydrophobic mismatch between phosphatidylcholine bilayers and transmembrane alpha-helical peptides depend on the nature of interfacially exposed aromatic and charged residues. Biochemistry. 2002; 41:8396–8404. [PubMed: 12081488]
11. van der Wel PC, Strandberg E, Killian JA, Koeppe RE 2nd. Geometry and intrinsic tilt of a tryptophan-anchored transmembrane alpha-helix determined by ^{2}H NMR. Biophys J. 2002; 83:1479–1488. [PubMed: 12202373]
12. Lee J, Im W. Transmembrane helix tilting: insights from calculating the potential of mean force. Phys Rev Lett. 2008; 100:018103. [PubMed: 18232823]
13. Vostrikov VV, Grant CV, Daily AE, Opella SJ, Koeppe RE 2nd. Comparison of "Polarization inversion with spin exchange at magic angle" and "geometric analysis of labeled alanines" methods for transmembrane helix alignment. J Am Chem Soc. 2008; 130:12584–12585. [PubMed: 18763771]
14. Vostrikov VV, Daily AE, Greathouse DV, Koeppe RE 2nd. Charged or aromatic anchor residue dependence of transmembrane peptide tilt. J Biol Chem. 2010; 285:31723–31730. [PubMed: 20667827]

15. Marassi FM, Opella SJ. A solid-state NMR index of helical membrane protein structure and topology. J Magn Reson. 2000; 144:150–155. [PubMed: 10783285]
16. Wang J, Denny J, Tian C, Kim S, Mo Y, Kovacs F, Song Z, Nishimura K, Gan Z, Fu R, Quine JR, Cross TA. Imaging membrane protein helical wheels. J Magn Reson. 2000; 144:162–167. [PubMed: 10783287]
17. Hall BA, Armitage JP, Sansom MSP. Transmembrane Helix Dynamics of Bacterial Chemoreceptors Supports a Piston Model of Signalling. PLOS Comput Biol. 2011; 7:e1002204. [PubMed: 22028633]
18. Kirchberg K, Kim TY, Moller M, Skegro D, Raju GD, Granzin J, Buldt G, Schlesinger R, Alexiev U. Conformational dynamics of helix 8 in the GPCR rhodopsin controls arrestin activation in the desensitization process. Proc Natl Acad Sci, USA. 2011; 108:18690–18695. [PubMed: 22039220]
19. Thomas R, Vostrikov VV, Greathouse DV, Koeppe RE 2nd. Influence of proline upon the folding and geometry of the WALP19 transmembrane peptide. Biochemistry. 2009; 48:11883–11891. [PubMed: 19891499]
20. Pace CN, Vajdos F, Fee L, Grimsley G, Gray T. How to measure and predict the molar absorption coefficient of a protein. Protein Sci. 1995; 4:2411–2423. [PubMed: 8563639]
21. Davis JH, Jeffrey KR, Bloom M, Valic MI, Higgs TP. Quadrupolar echo deuteron magnetic resonance spectroscopy in ordered hydrocarbon chains. Chem Phys Lett. 1976; 42:390–394.
22. Wu CH, Ramamoorthy A, Opella SJ. High-Resolution Heteronuclear Dipolar Solid-State NMR Spectroscopy. J Magn Reson A. 1994; 109:270–272.
23. Nevzorov AA, Opella SJ. A “magic sandwich” pulse sequence with reduced offset dependence for high-resolution separated local field spectroscopy. J Magn Reson. 2003; 164:182–186. [PubMed: 12932472]
24. Cook GA, Opella SJ. NMR studies of p7 protein from hepatitis C virus. Eur Biophys J. 2010; 39:1097–104. [PubMed: 19727701]
25. Nevzorov AA, Opella SJ. Selective averaging for high-resolution solid-state NMR spectroscopy of aligned samples. J Magn Reson. 2007; 185:59–70. [PubMed: 17074522]
26. Triba MN, Warschawski DE, Devaux PF. Reinvestigation by Phosphorus NMR of Lipid Distribution in Bicelles. Biophys J. 2005; 88:1887–1901. [PubMed: 15626702]
27. Vostrikov VV, Grant CV, Opella SJ, Koeppe RE 2nd. On the Combined Analysis of ^{2}H and ^{15}N/^{1}H Solid-State NMR Data for Determination of Transmembrane Peptide Orientation and Dynamics. Biophys J. 2011; 101:2939–2947. [PubMed: 22208192]
28. van der Wel PCA, Reed ND, Greathouse DV, Koeppe RE 2nd. Orientation and Motion of Tryptophan Interfacial Anchors in Membrane-Spanning Peptides. Biochemistry. 2007; 46:7514–7524. [PubMed: 17530863]
29. Gleason, NJ.; Vostrikov, VV.; Koeppe, RE, 2nd. Comparison of Mechanical and Magnetic Alignment of WALP-like Peptides for Solid-State NMR. Biophys J; 2009; Biophysical Society Meeting Abstracts; 2009. p. 445ap. Abstract, 2349-Pos
30. Strandberg E, Esteban-Martin S, Salgado J, Ulrich AS. Orientation and dynamics of peptides in membranes calculated from ^{2}H-NMR data. Biophys J. 2009; 96:3223–3232. [PubMed: 19383466]
31. Strandberg E, Ozdirekcan S, Rijkers DT, van der Wel PC, Koeppe RE 2nd, Liskamp RM, Killian JA. Tilt angles of transmembrane model peptides in oriented and non-oriented lipid bilayers as determined by ^{2}H solid-state NMR. Biophys J. 2004; 86:3709–3721. [PubMed: 15189867]
32. Nevzorov AA, Mesleh MF, Opella SJ. Structure determination of aligned samples of membrane proteins by NMR spectroscopy. Magn Reson Chem. 2004; 42:162–171. [PubMed: 14745796]
33. Saito H, Ando I, Ramamoorthy A. Chemical shift tensor - the heart of NMR: Insights into biological aspects of proteins. Prog Nucl Magn Reson Spectrosc. 2010; 57:181–228. [PubMed: 20633363]
34. Bechinger B, Resende JM, Aisenbrey C. The structural and topological analysis of membrane-associated polypeptides by oriented solid-state NMR spectroscopy: established concepts and novel developments. Biophys Chem. 2011; 153:115–125. [PubMed: 21145159]
35. Ketchem RR, Lee KC, Huo S, Cross TA. Macromolecular structural elucidation with solid-state NMR-derived orientational constraints. J Biomol NMR. 1996; 8:1–14. [PubMed: 8810522]

36. Tian C, Gao PF, Pinto LH, Lamb RA, Cross TA. Initial structural and dynamic characterization of the M2 protein transmembrane and amphipathic helices in lipid bilayers. Protein Sci. 2003; 12:2597–2605. [PubMed: 14573870]
37. Vostrikov, VV. PhD Dissertation. University of Arkansas; 2011.
38. Killian JA, Taylor MJ, Koeppe RE 2nd. Orientation of the valine-1 side chain of the gramicidin transmembrane channel and implications for channel functioning. A ^{2}H NMR study. Biochemistry. 1992; 31:11283–11290. [PubMed: 1280159]
39. Ozdirekcan S, Etchebest C, Killian JA, Fuchs PF. On the orientation of a designed transmembrane peptide: toward the right tilt angle? J Am Chem Soc. 2007; 129:15174–15181. [PubMed: 18001020]
40. Esteban-Martin S, Salgado J. The dynamic orientation of membrane-bound peptides: bridging simulations and experiments. Biophys J. 2007; 93:4278–4288. [PubMed: 17720729]
41. Strandberg E, Esteban-Martin S, Ulrich AS, Salgado J. Hydrophobic mismatch of mobile transmembrane helices: Merging theory and experiments. Biochim Biophys Acta. 2012; xxx in press. 10.1016/j.bbamem.2012.01.023
42. Ren J, Lew S, Wang Z, London E. Transmembrane orientation of hydrophobic alpha-helices is regulated both by the relationship of helix length to bilayer thickness and by the cholesterol concentration. Biochemistry. 1997; 36:10213–10220. [PubMed: 9254619]
43. Vostrikov VV, Hall BA, Greathouse DV, Koeppe RE 2nd, Sansom MSP. Changes in Transmembrane Helix Alignment by Arginine Residues Revealed by Solid-State NMR Experiments and Coarse-Grained MD Simulations. J Am Chem Soc. 2010; 132:5803–5811. [PubMed: 20373735]
44. Monticelli L, Tieleman DP, Fuchs PF. Interpretation of ^{2}H-NMR experiments on the orientation of the transmembrane helix WALP23 by computer simulations. Biophys J. 2010; 99:1455–1464. [PubMed: 20816057]
45. Holt A, Rougier L, Reat V, Jolibois F, Saurel O, Czaplicki J, Killian JA, Milon A. Order parameters of a transmembrane helix in a fluid bilayer: case study of a WALP peptide. Biophys J. 2010; 98:1864–1872. [PubMed: 20441750]
46. DeLano, WL. The PyMOL Molecular Graphics System. 2002.
47. Pulay P, Scherer EM, van der Wel PC, Koeppe RE 2nd. Importance of tensor asymmetry for the analysis of ^{2}H NMR spectra from deuterated aromatic rings. J Am Chem Soc. 2005; 127:17488–17493. [PubMed: 16332101]

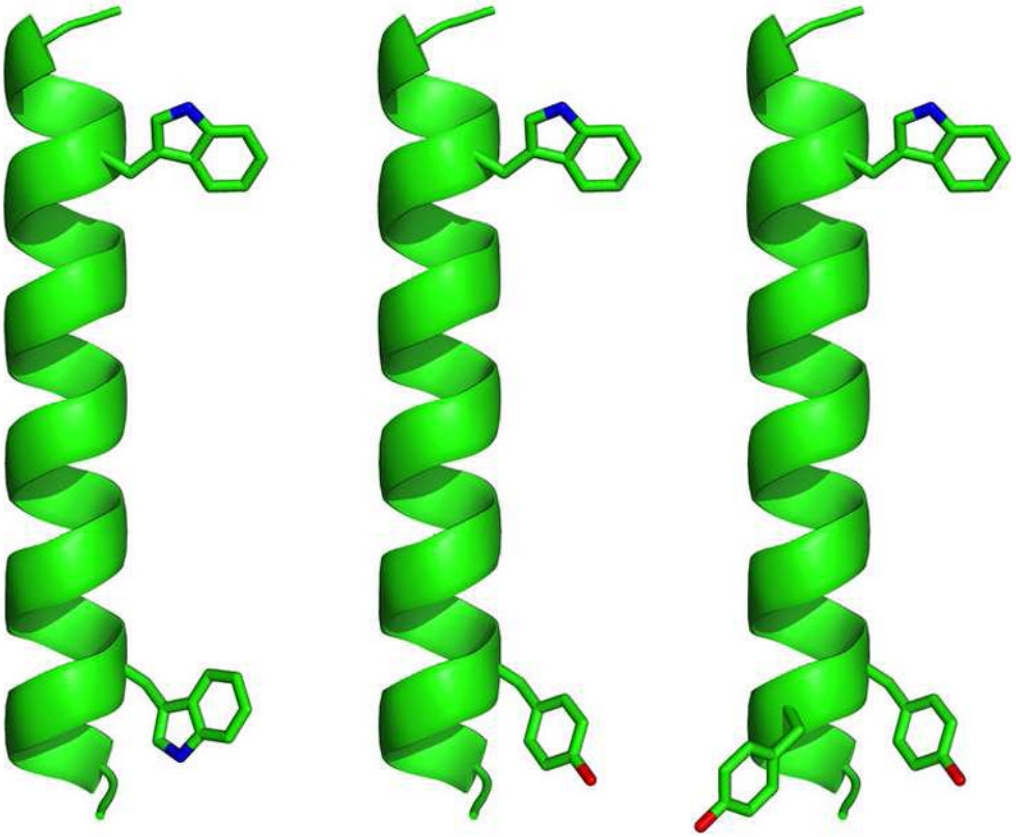

Figure 1.
Representative models of GWALP23, Y^{5}GWALP23, and $Y^{4,5}$GWALP23 (left to right), showing the locations of aromatic side chains on a ribbon helix, drawn using PyMOL (46). The side-chain orientations are arbitrary.

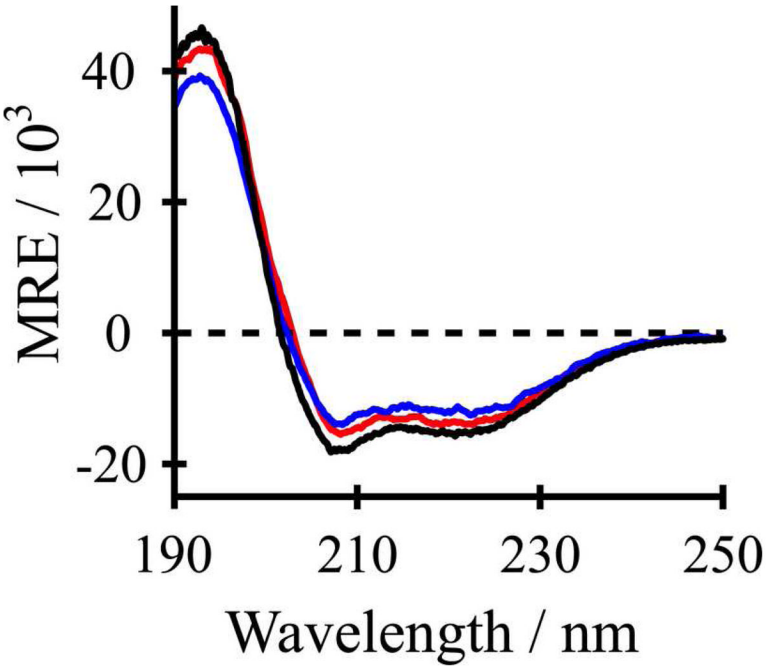

Figure 2.
Circular dichroism spectra of GWALP23 (black), Y^{5}GWALP23 (blue) and $Y^{4,5}$GWALP23 (red) in DLPC vesicles.

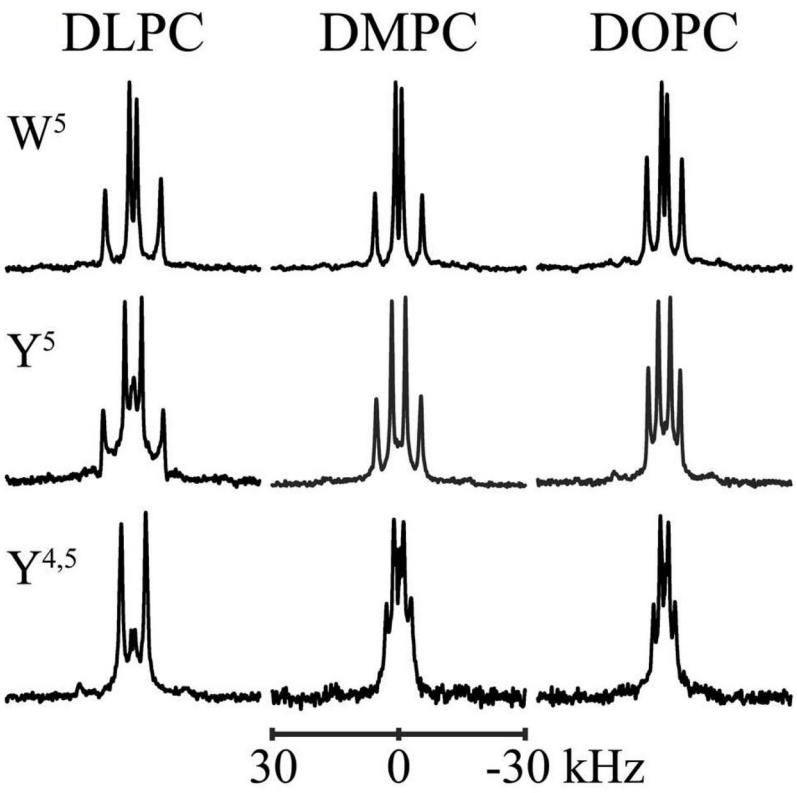

Figure 3.
^{2}H NMR spectra of (top to bottom) GWALP23, Y^{5}GWALP23, and Y^{4,5}GWALP23, each labeled at Ala^{17} (100% ^{2}H) and Ala^{7} (60% ^{2}H), in hydrated oriented bilayers of DLPC, DMPC and DOPC. Peptide/lipid ratio, 1/60 (mol/mol); 50 °C; β = 90° sample orientation.

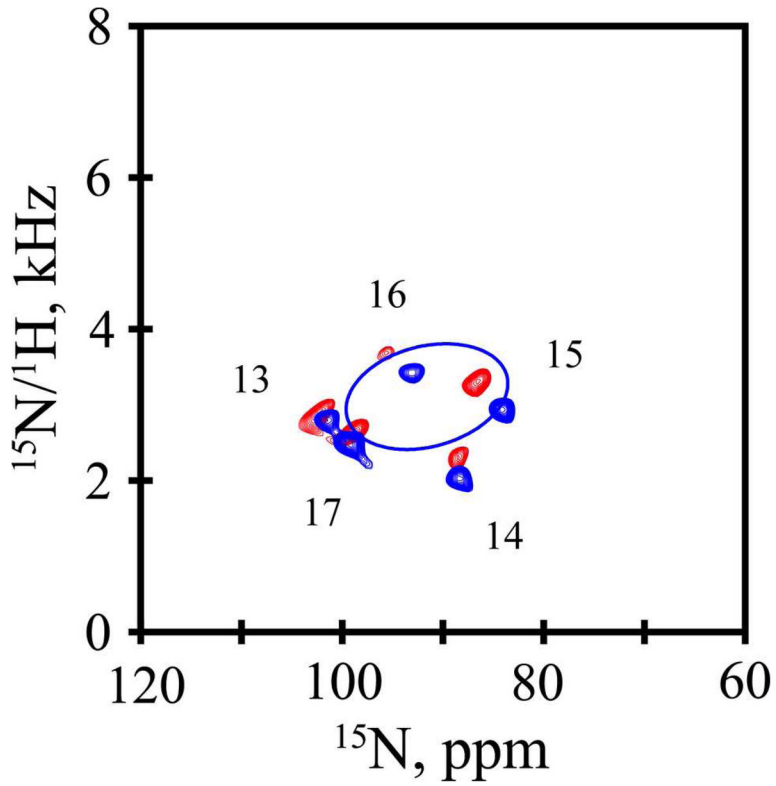

Figure 4.

SAMPI4 spectra, with assignments, for GWALP23 (red) and Y^{5}GWALP23 (blue, with PISA wheel corresponding to the combined fit to ^{15}N and ^{2}H data, Table 4), each ^{15}N labeled in residues 13–17. Peptide/lipid ratio, 1/80 (mol/mol); 42 °C; bicelles of DMPC/DHPC (q = 3.2).

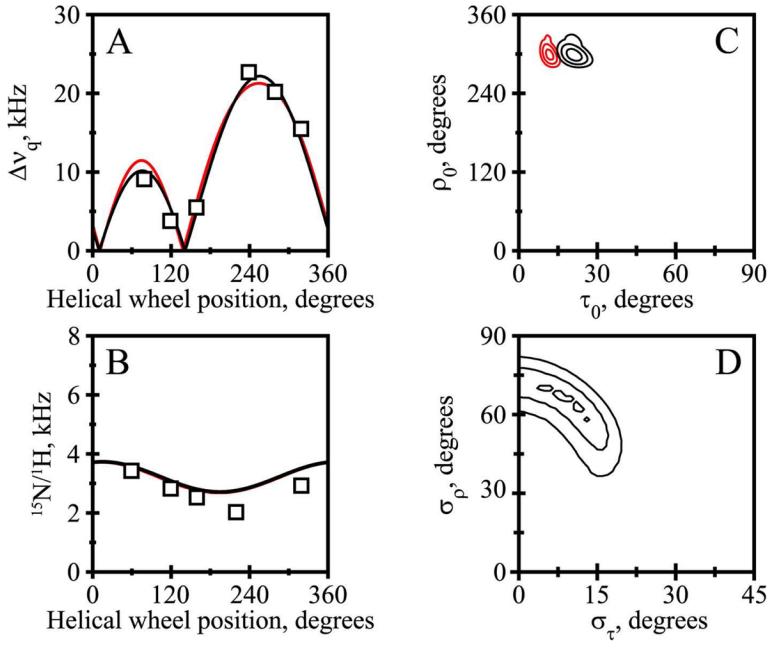

Figure 5.

Combined ^{15}N and ^{2}H analysis for Y^{5}GWALP23 in DMPC. A. Quadrupolar waves from Gaussian dynamics (black curve) and semi-static (red curve) analysis. B. Dipolar waves from Gaussian (black curve) and semi-static (red curve) analysis. C. RMSD (τ_o, ρ_o) graph for the Gaussian (black contours) and semi-static (red contours) analyses, contoured at 1.5, 2.0 and 2.5 kHz. D. RMSD (σ_τ, σ_ρ) graph for the Gaussian dynamics analysis, contoured at 0.95, 1.15 and 1.35 kHz.

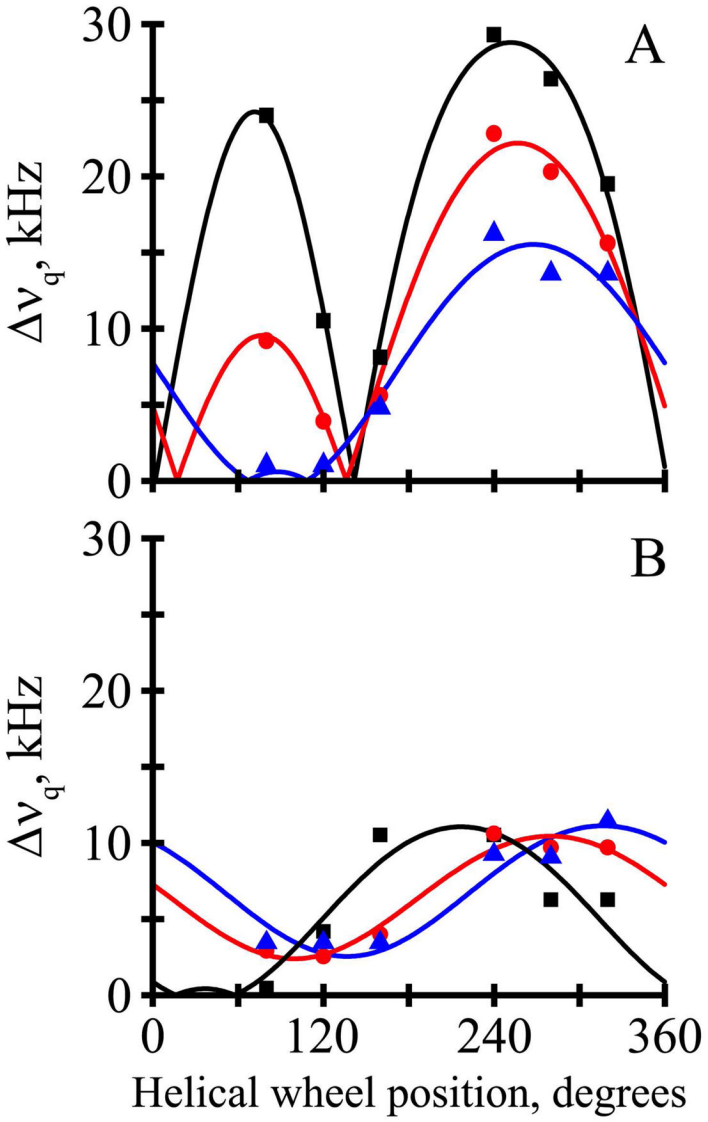

Figure 6.
GALA semi-static analysis of Ala-d_4 quadrupolar splittings using variable S_{zz} (see (11)). Quadrupolar wave plots are shown for Y^5GWALP23 (A) and $Y^{4,5}$GWALP23 (B) in oriented bilayers of DLPC (black squares), DMPC (red circles) and DOPC (blue triangles). Fitted curves represent theoretical $\Delta\nu_q$ values for orientations corresponding to best-fit values of τ_o and ρ_o.

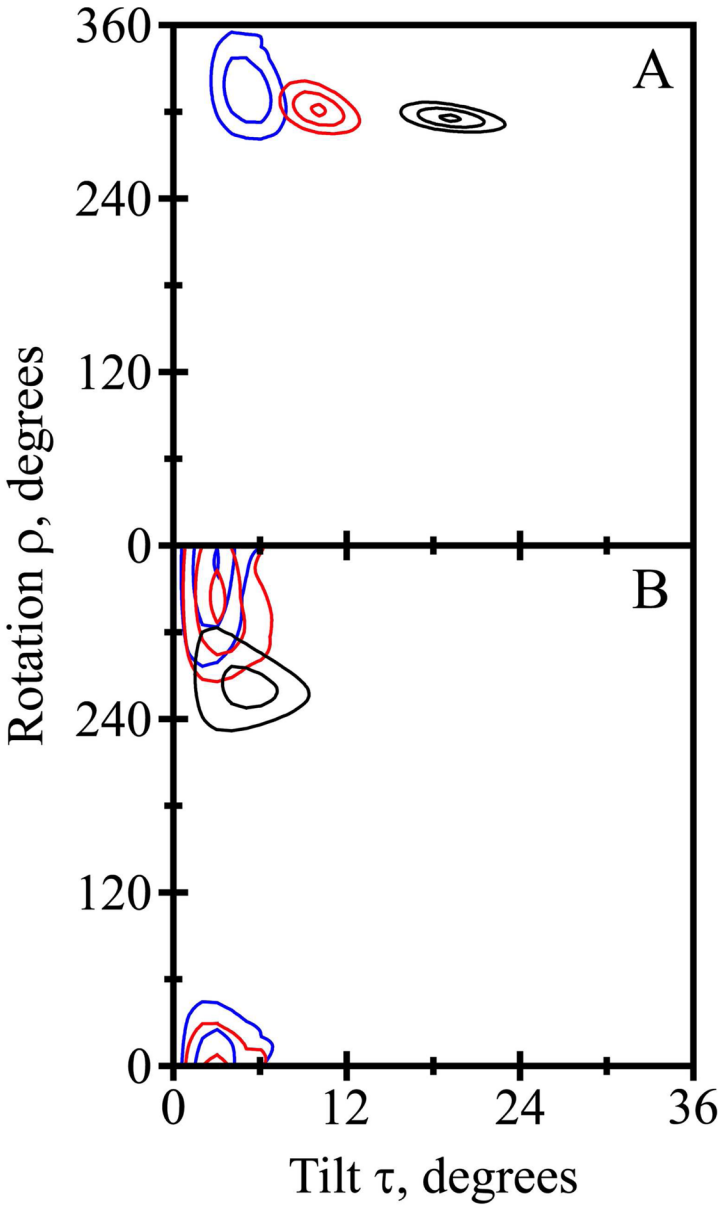

Figure 7.

RMSD contour plots for apparent average tilt τ_o and rotation ρ_o resulting from semi-static GALA analysis of Y^5GWALP23 (A) and $Y^{4,5}$GWALP23 (B) in DLPC (black), DMPC (red), and DOPC (blue). Contour levels are drawn at 1, 2, and 3 kHz.

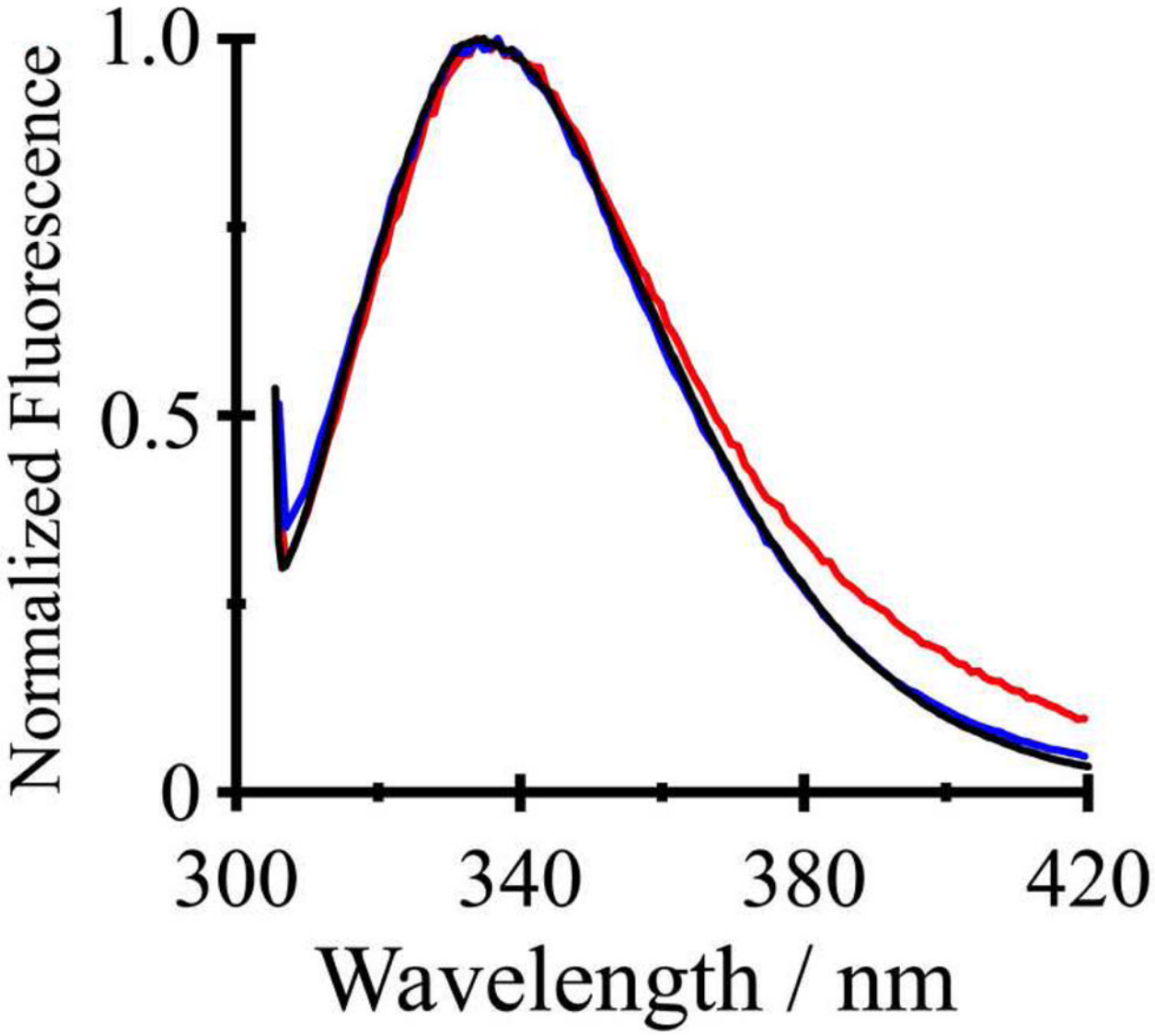

Figure 8.
Steady-state fluorescence spectra of GWALP23 (black), Y^{5}GWALP23 (blue) and $Y^{4,5}$GWALP23 (red) in DLPC vesicles excited at 295 nm.

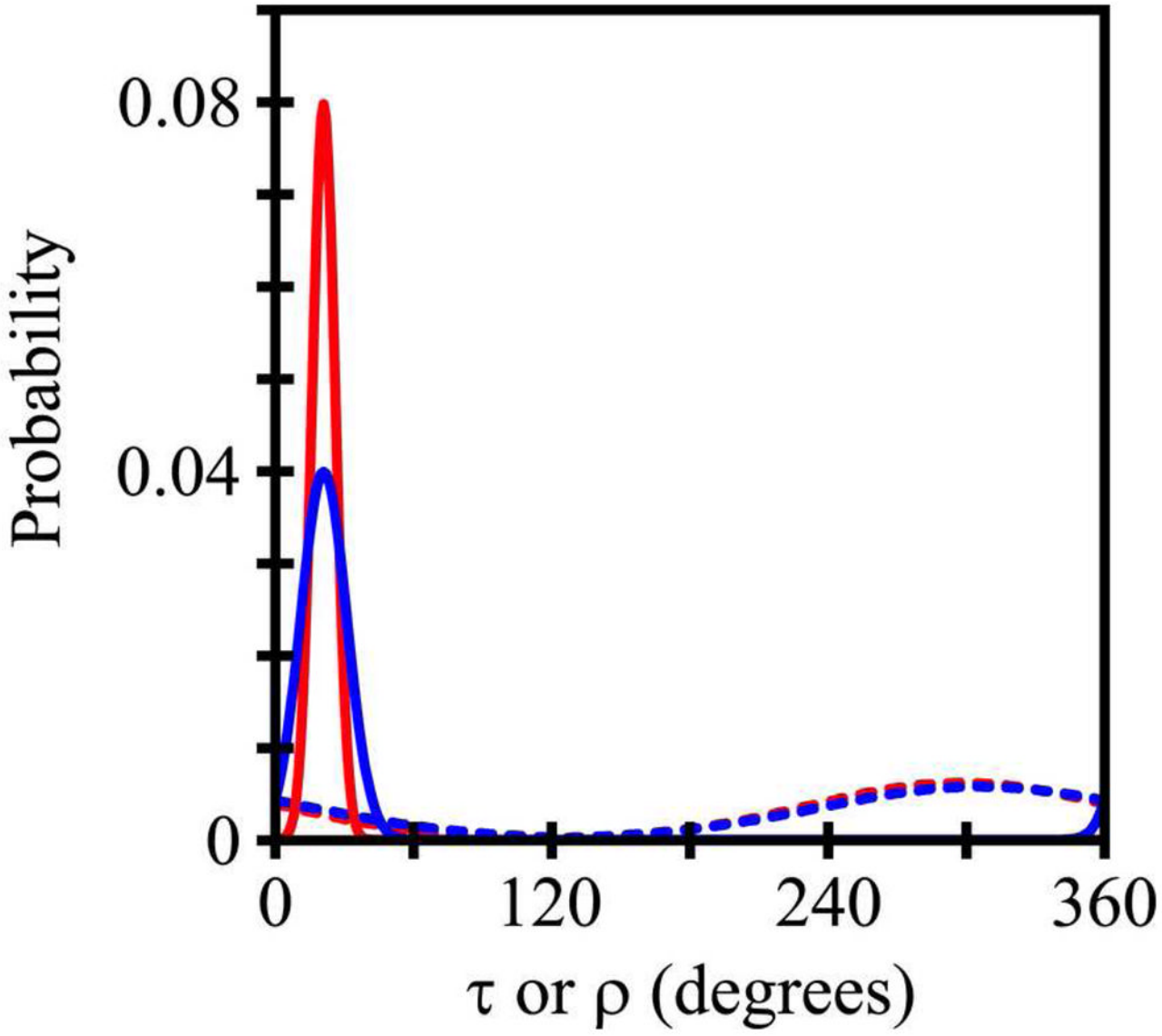

Figure 9.

Curves to indicate the widths of the τ distributions (solid curves) and ρ distributions (dashed curves) for GWALP23 (red) and Y^5GWALP23 (blue), based on Gaussian dynamics analysis of combined GALA and SAMPI4 measurements for each peptide in DMPC.

Table 1

Sequences of GWALP23 and related peptides[a]

Name	Sequence
WALP23	a-GWW^{3}LALALALALALALALALWWA-e
WALP19	a-GWW^{3}LALALALALALALWWA-e
GWALP23	a-GGALW^{5}LALALALALALALWLAGA-e
Y^{5}GWALP23	a-GGALY^{5}LALALALALALALWLAGA-amide
Y^{4,5}GWALP23	a-GGAYY^{5}LALALALALALALWLAGA-amide

[a]Abbreviations: “a” denotes “acetyl” and “e” denotes “ethanolamide.”

Table 2

Observed ^{2}H quadrupolar splittings[a] for GWALP23[b] and Tyr-based analogues in three lipids.

	DLPC			DMPC			DOPC		
Residue	**$W^{5,19}$**	**$Y^{5}W^{19}$**	**$Y^{4,5}W^{19}$**	**$W^{5,19}$**	**$Y^{5}W^{19}$**	**$Y^{4,5}W^{19}$**	**$W^{5,19}$**	**$Y^{5}W^{19}$**	**$Y^{4,5}W^{19}$**
7	26.4	29.3	11.6	21.9	22.8	11.7	16.6	16.2	10.2
9	25.5	24.0	0.5	8.9	9.2	3.2	1.7	0.5	3.8
11	26.9	26.4	6.9	20.9	20.3	10.7	16.7	13.6	10.0
13	14.6	10.5	4.6	3.8	3.9	2.8	1.5	0.5	3.8
15	20.7	19.5	6.9	17.6	15.6	10.7	15.4	13.6	12.6
17	3.4	8.1	11.6	2.9	5.6	4.4	2.6	4.8	3.8

[a] Quadrupolar splittings are reported in kHz for the β = 0° sample orientation of GWALP23 (having W5 and W19), Y^{5}GWALP23, and $Y^{4,5}$GWALP23. Each value is an average of (the magnitude observed when β = 0°), and (twice the magnitude observed when β = 90°).

[b] Values for GWALP23 from (14). The positions of the aromatic residues in the peptides are listed as $W^{5,19}$, $Y^{5}W^{19}$ and $Y^{4,5}W^{19}$.

Table 3

Dipolar couplings and ^{15}N chemical shift values for peptide $^{15}N/^{1}H$ groups[a]

	GWALP23		Y^{5}GWALP23	
Residue	**^{15}N, ppm**	**$^{15}N/^{1}H$, kHz**	**^{15}N, ppm**	**$^{15}N/^{1}H$, kHz**
13	101	3.0	101	2.8
14	87	2.4	88	2.0
15	85	3.4	84	2.9
16	94	3.8	93	3.4
17	97	2.8	99	2.5

Values were measured in DMPC/DHPC bicelles and correspond to a β = 90° sample orientation.

Table 4

Calculated orientations and dynamics of peptides in DMPC and DLPC[a]

Peptide	Lipid	Model	τ_0	σ_τ	ρ_0	σ_ρ	S_{zz}	RMSD (kHz)	n[b]
GWALP23	DMPC	Gaussian	21°	5°	306°	70°	0.88[c]	1.1	16
	DMPC	semi-static	11°	n.a.[d]	307°	n.a.[d]	0.75	1.2	16
Y^5GWALP23	DMPC	Gaussian	21°	9°	298°	66°	0.88[c]	1.2	16
	DMPC	semi-static	12°	n.a.[d]	298°	n.a.[d]	0.73	1.2	16
GWALP23	DLPC	Gaussian	23°	15°	304°	33°	0.88[c]	0.7	6
	DLPC	semi-static	21°	n.a.[d]	305°	n.a.[d]	0.71	0.7	6
Y^5GWALP23	DLPC	Gaussian	21°	12°	295°	27°	0.88[c]	0.7	6
	DLPC	semi-static	19°	n.a.[d]	295°	n.a.[d]	0.78	0.7	6
$Y^{4,5}$GWALP23	DLPC	Gaussian	11°	27°	261°	60°	0.88[c]	1.5	6
	DLPC	semi-static	5°	n.a.[d]	260°	n.a.[d]	0.66	1.6	6

[a] The Gaussian model for the dynamics uses a fixed principal order parameter S_{ZZ} (30), representing the dynamic extent of (mis)alignment (angle α) between the molecular *z*-axis and its average orientation, characterized by the time average $S_{ZZ} = \langle 3\cos^2\alpha - 1\rangle/2$ (47). Within this context, further motions can be characterized by the widths σ_τ and σ_ρ of Gaussian distributions about the average values of tilt magnitude τ_0 and tilt direction ρ_0 (30). An alternative semi-static analysis, using three parameters instead of four, determines the best fit (lowest RMSD, in kHz) as a function of τ_0, ρ_0 and a variable S_{ZZ}.

[b] Number of data points (from Tables 2–3), identified as six ^{2}H methyl quadrupolar couplings, either alone or with five ^{15}N/^{1}H dipolar couplings and ^{15}N chemical shifts.

[c] Fixed value.

[d] Not applicable.

Table 5

Semi-static GALA analysis of GWALP23 and Tyr-anchored analogues[a]

	DLPC				DMPC				DOPC			
Aromatic residues	**τ_0**	**ρ_0**	**S_{zz}**	**RMSD (kHz)**	**τ_0**	**ρ_0**	**S_{zz}**	**RMSD (kHz)**	**τ_0**	**ρ_0**	**S_{zz}**	**RMSD (kHz)**
b $W^{5,19}$	21°	305°	0.71	0.7	9°	311°	0.88	1.0	6°	323°	0.87	0.6
Y^5W^{19}	19°	295°	0.78	0.7	10°	300°	0.84	0.7	5°	311°	0.84	1.0
$Y^{4,5}W^{19}$	5°	260°	0.66	1.6	3°	323°	0.77	0.6	3°	359°	0.82	1.1

[a] Calculations based on six Ala methyl ^2H quadrupolar splittings only. The reduced S_{ZZ} values, variable apparent ρ_O values and low apparent τ_O values render $Y^{4,5}$GWALP23 the outlier among this set of peptides.

[b] Values for GWALP23 from reference (14).